

A PRE-MERGER IN THE LUMINOUS INFRARED SYSTEM IRAS 02290+2533

Fidel Cruz¹ and Héctor Aceves²

Received 2008 October 21; accepted 2009 August 3

RESUMEN

Reportamos imágenes y fotometría obtenidas en el óptico y cercano infrarrojo, de la fuente IRAS 02290+2533. Las observaciones muestran que esta fuente es un sistema de tres galaxias. Dos galaxias (A y B), cuya separación proyectada es de ≈ 10 kpc, muestran evidencias de una interacción de marea entre ellas. La galaxia tipo espiral B presenta una emisión extendida en $H\alpha$ y una luminosidad infrarroja alta, desde longitudes de onda cercanas a medias. Sugerimos que tal luminosidad se debe a un brote de formación estelar, que abarca probablemente casi todo el disco, originado por la interacción gravitacional en curso con la galaxia A. La galaxia B puede ser clasificada como una Galaxia Infrarroja Luminosa (LIRG). Estimamos que una fusión binaria de galaxias puede ocurrir en el sistema dentro de $\lesssim 1$ Gyr. Es probable que esta fuente IRAS albergue en un futuro una galaxia Ultra LIRG, en concordancia con el modelo evolutivo de Sanders & Mirabel (1996).

ABSTRACT

We report optical and near-infrared imaging and photometry for the IRAS 02290+2533 source. Observations show that this source is a system of three galaxies. Two galaxies (A and B), which are separated in projection ≈ 10 kpc, show some evidence of tidal interaction between them. The spiral-like Galaxy B presents a disk-wide $H\alpha$ emission and a high infrared luminosity, from near to mid-infrared wavelengths. We suggest that such luminosity is due to a probable disk-wide starburst triggered by the ongoing gravitational interaction with Galaxy A. Galaxy B can be classified as a Luminous Infrared Galaxy (LIRG). We estimate that a binary merger in the system is likely to occur in $\lesssim 1$ Gyr. It is probable that this IRAS source will harbor in the future an Ultra LIRG, according to the evolutionary scheme of Sanders & Mirabel (1996).

Key Words: galaxies: interactions — galaxies: photometry — infrared: galaxies — infrared: general

1. INTRODUCTION

One of the most important results from the Infrared Astronomy Satellite (IRAS; Neugebauer et al. 1984) mission was the discovery of a new type of galaxies, namely: the luminous infrared galaxies (LIRGs) and the ultraluminous infrared galaxies (ULIRGs) (e.g. Soifer et al. 1984; Sanders & Mirabel 1996; Lonsdale et al. 2006). These galaxies are characterized by a strong emission at mid and far-infrared wavelengths (8–1000 μ) with luminosities $L_{\text{fir}} \gtrsim 10^{11} L_{\odot}$. The most powerful emit-

ters are the ULIRGs, with bolometric luminosities $L_{\text{fir}} \gtrsim 10^{12} L_{\odot}$, that lie in a range comparable to that of quasars. Optical and near-IR studies of LIRGs and ULIRGs show that they are associated with strong tidal interactions or are undergoing a merger (e.g. Armus, Heckman, & Miley 1987; Sanders et al. 1988; Carico et al. 1990; Murphy et al. 1996; Veilleux, Kim, & Sanders 2002).

Disk galaxy interactions are known to trigger extensive starbursts events (e.g. Sulentic 1989; Mihos & Hernquist 1996; Schweizer 1998). Massive OB stars dominate the flux of the starburst in the optical and ultraviolet wavelengths. The gas and dust surrounding the starburst reprocess such radiation

¹Bahía San Quintín, Ensenada, B. C., Mexico.

²Instituto de Astronomía, Universidad Nacional Autónoma de México, Ensenada, B. C., Mexico.

and re-emit it at infrared (IR) wavelengths. The high luminosity in IR wavelengths is a clear indication of an episode of recent star formation activity in galaxies (e.g. Lonsdale, Persson, & Mathews 1984; Telesco 1988; Canalizo & Stockton 2001). Optical and near-IR spectroscopic surveys have shown that LIRGs and ULIRGs can be classified as luminous starburst and/or active galactic nuclei (AGNs; Sanders et al. 1988; Armus et al. 1987; Veilleux, Sanders, & Kim 1999; Dasyra et al. 2006).

Sanders et al. (1988) suggested that ULIRGs would evolve eventually to quasars (QSOs). In general, it is proposed that massive star formation induced by the gravitational interactions would create a compact cluster of stars, that eventually will lead to the formation of a massive black hole. This black hole will be fed by neighboring material and in turn, lead to the formation of a quasar. The details of the transformation from ULIRGs to QSOs are not completely understood (e.g. Genzel et al. 2001), but observations suggest that most luminous ULIRGs are the precursors of QSOs (Veilleux et al. 1995; Veilleux, Sanders, & Kim 1997; Lutz, Veilleux, & Genzel 1999) and theoretical models lend support to this idea (e.g. Hopkins et al. 2006).

From a series of studies of Surace and coworkers (e.g. Surace et al. 1998; Surace & Sanders 1999; Surace, Sanders, & Evans 2000) a morphological classification of ULIRGs according to different stages of evolution is proposed: (i) pre-contact; (ii) first contact with no visible tidal tails; (iii) pre-merger with tidal tails and double nuclei separated by (a) more than 10 kpc, and (b) less than 10 kpc; (iv) merger with long tidal tails and a single (a) diffuse, and (b) compact nucleus; and (v) final configuration of a merger with no tidal tails and strong central activity. The LIRGs phase is mostly associated with the initial stages of the gravitational interaction, while the ULIRGs phase is thought to occur near the complete fusion of the disk galaxy progenitors (e.g. Kormendy & Sanders 1992; Sanders & Mirabel 1996).

The IRAS 02290+2533 source is a relatively poorly studied system; only 3 references (Strauss et al. 1992; Lu & Freudling 1995; Yun, Reddy, & Condon 2001) to this source are found in NED,³ and no detailed study of this system appears to exist. The redshift for the source is $z = 0.051$ (Strauss et al. 1992), that places it at a comoving radial distance of $D \approx 216$ Mpc in a Λ CDM cosmology with $H_0 = 70 \text{ km s}^{-1}$. At this distance, about 1 kpc corresponds to ≈ 1 arcsec. This source has a luminosity of

³NASA/IPAC Extragalactic Database.

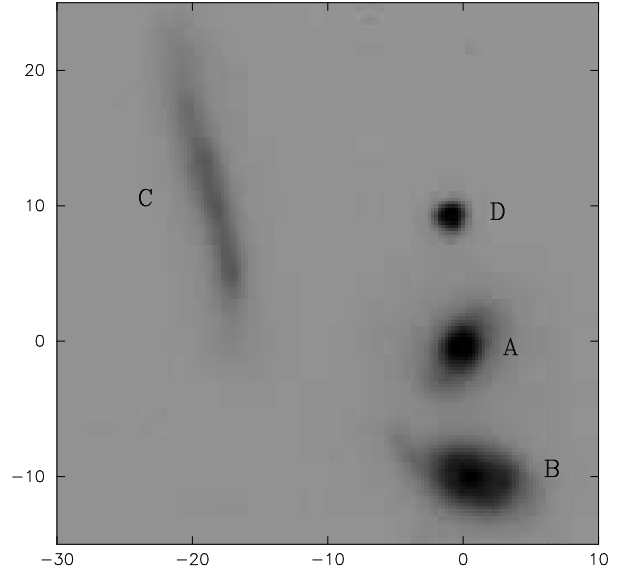


Fig. 1. Optical image in the broad-band filter R of the IRAS 02290+2533 source. The main galaxies in the system are labeled A, B and C. North is on the top and east to the left. Axis scale is in arcsec. Object D is apparently a star.

$\log(L_{\text{ir}}) = 11.63$ and a color index of $f_{25}/f_{60} = 0.11$, where f_{λ} is the flux density at wavelength $\lambda(\mu\text{m})$. This luminosity places the source in the upper range of the LIRGs classification.

A NED search identifies this IRAS source with two galaxies in the 2MASX archive: J02315405 + 2546187 and J02315405 + 2546087 for the north (A) and south (B) galaxies, respectively (see Figure 1). In this work an additional source (Galaxy C) is identified in the field of this infra-red source.

The purpose of this work is to examine the morphology of the IRAS 02290+2533 source, and to classify it using data from the optical and IR wavelengths. Also, we explore the possibility that this system is at an initial pre-merger stage that will eventually evolve into an elliptical galaxy as proposed by Sanders et al. (1988) and Sanders (2004). We present V , R , I , $H\alpha$ optical and near-IR J , H , and K' images, and photometry of the galaxies in the field of IRAS 02290+2533.

The rest of the paper has been organized as follows. In § 2 we present details of our optical and near-IR observations. Results and a discussion are provided in § 3 and § 4, respectively.

2. OBSERVATIONS

2.1. Optical

Optical observations were carried out with the 1.5 m telescope in San Pedro Mártir, Baja California,

TABLE 1
OPTICAL AND NEAR IR PHOTOMETRY RESULTS

Galaxy	V	R	J	H	K'
A	16.66 ± 0.03	16.15 ± 0.04	14.22 ± 0.06 (14.12 ± 0.05)	13.45 ± 0.02 (13.23 ± 0.05)	12.64 ± 0.02 (12.88 ± 0.07)
B	16.44 ± 0.03	15.75 ± 0.04	13.49 ± 0.06 (13.55 ± 0.03)	12.71 ± 0.02 (12.71 ± 0.04)	11.90 ± 0.02 (12.23 ± 0.05)
C			14.25 ± 0.9	13.31 ± 0.9	

Data from 2MASX is shown in parenthesis for comparison.

México, operated by the Observatorio Astronómico Nacional (OAN/SPM) on August 16–17 of 1999. We used a 1024×1024 Thompson CCD detector with a broad band Johnson-Cousins $BVRI$ photometric system, and narrow-band redshifted $H\alpha$ centered at 692 nm ($\Delta\lambda = 10$ nm). The detector scale gives a spatial resolution of $0.25''/\text{pix}$ yielding a field of view of $2'.56 \times 2'.56$.

Reductions and analysis were made in the usual way using with the IRAF environment package. The sky flats were obtained at sunset. Total integration time was 1200s and 900s for broad band filters and narrow band filter, respectively. Seeing conditions were $1.2'' - 1.5''$ during these observations with a FWHM of $1.5''$. The nights were photometric. A photometric calibration was done using standard stars SA114-654 and SA114-656 in the V and R filters. Errors come from the procedure to obtain instrumental magnitudes, and no correction for extinction was made.

2.2. Near-IR

Near-IR observations were obtained with a NICMOS array of 256×256 pixels, with a $0.8''/\text{pix}$ plate scale and a field of view of $1.2' \times 1.2'$ (Cruz-González et al. 1994) at the 2.1 m telescope of the OAN/SPM. Images were taken under photometric conditions on July 29–30 of 1999 through the broad band filters J ($1.20 \mu\text{m}$, $\Delta\lambda = 0.28 \mu\text{m}$), H ($1.60 \mu\text{m}$, $\Delta\lambda = 0.27 \mu\text{m}$), and K' ($2.125 \mu\text{m}$, $\Delta\lambda = 0.35 \mu\text{m}$). Five added object images were processed by subtraction of median-filtered images of four nearby sky frames taken with the same exposure times at positions adjacent to the object. The total integration time (summing all expositions for each filter) was 300s for each image filter. The images were flattened by low and high illumination sky flats obtained at sunset.

The faint standard stars FS4 and FS125 from *UKIRT* were observed in order to calibrate near-IR observations. Each standard star was measured

with the same observational procedure as the galaxies, and repeated three times each night. All these observations were combined to determine the zero-point offset. Principal extinction coefficients were taken from Carrasco et al. (1991).

The main source of the errors come from the procedure to obtain the instrumental magnitudes. Total conservative uncertainties for each band are reported in Table 1.

3. RESULTS

3.1. Morphology

Figure 1 shows the main bright objects comprising the field of view of the IRAS source in the R -band and are labeled as A, B, C and D. We identify objects A, B and C as a galaxies. According to the IRAF analysis of the light profile of D, this object appears to have a profile consistent with that of a star; hence we do not consider it further in this work.

Images for each galaxy in the $H\alpha$, V , R and I filters are shown in Figure 2. Near-IR J , H and K' filters for each galaxy are also presented in Figure 3. Position angles (PA) and ellipticities from the IRAF surface package are reported in Figure 4, in the H and J filters.

Galaxy A was taken as center of the field. The other galaxies in the field are B and C, being at $10''$ and $25''$ from A galaxy to the south and the north-east directions respectively. Figures 2 and 3 show some morphological features in each filter, as well as corresponding isophotes.

Galaxy A displays the most round appearance in its central region and some isophote twist toward the outside. The PA (Figure 4) shows that the external twist is from the north-west (25–35 degrees in PA) to the south-east (205–215 degrees in PA) direction in the two filters shown. The extension of the twisted region may be taken to be about $2'' - 3''$. In the K' filter the image is rounder and in the $H\alpha$ filter

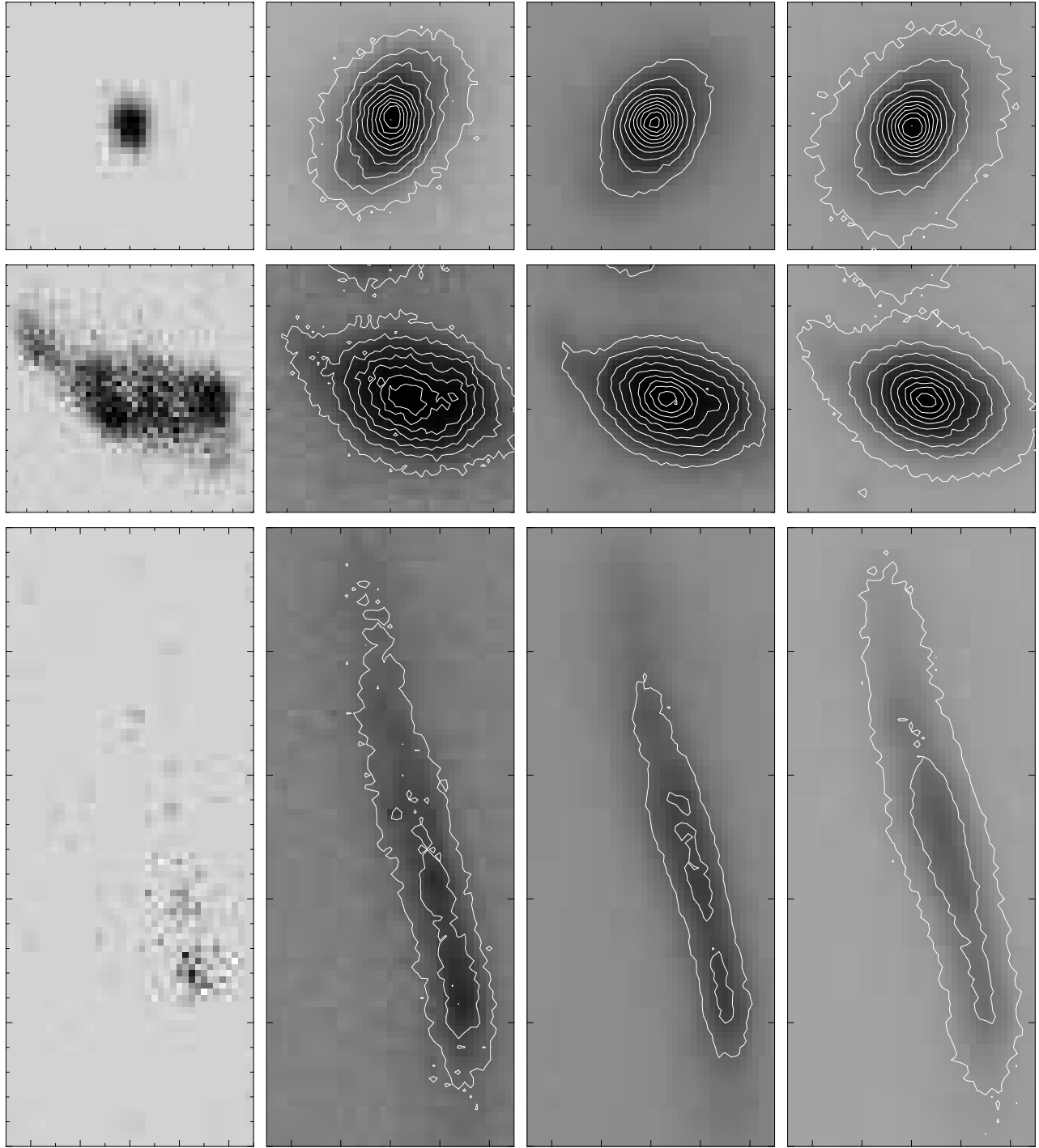


Fig. 2. Optical images (from left to right) in the narrow-band redshifted $H\alpha$ filter and the broad band filters V , R , I of the objects labeled A, B and C (from top, middle and bottom, respectively) in Figure 1.

appears more like a compact source. Ellipticity variation is rather small for this galaxy, with values of 0.15 in central region to 0.28 in the external region in the J band (see Figure 4).

Galaxy B shows an elongation of $\sim 10'' - 15''$ in all images in the east-west direction, and what resembles a tidal feature of an extension of $4'' - 5''$. An isophote twist pointing toward the north direc-

tion, i.e. pointing towards Galaxy A, is also noticed. Figure 4 shows a decreasing in PA of this “tidal feature” with radius, going from -75 degrees to -65 degrees. Ellipticity in the isophotes is stronger than in Galaxy A, going from about 0.25 to 0.37.

The $H\alpha$ emission from Galaxy B is coincident with the elongation shown in the broad band images. Some emission from knot-like structures of $\sim 2'' \times 2''$ is detected at each side of what may be considered its center (Figure 2; middle panel). Also a diminishing of the $H\alpha$ emission is observed in this central region.

Galaxy C appears to be a highly inclined spiral in all filter images. Unfortunately, no redshift value for this galaxy appears to exist, hence one cannot argue firmly in favour of its physical association with the IRAS source. On other hand, the absence of an obvious tidal features may lead to the idea that it may be a chance projection. Nonetheless, it could also be well in an early stage of interaction where the disk is not very perturbed, although its dark halo may be highly deformed. Furthermore, there is some indication shown in the images that its disk may be slightly warped. We consider here Galaxy C in physical association with the source.

This Galaxy C is rather faint in the V , R and I bands, with a little bright extension to the south; particularly in the $H\alpha$ image. The relative luminosity for this galaxy increases in the J and H filters, where the main emission comes from central region. The PA of the elongation axis of Galaxy C is about 70 degrees. The ellipticity of the isophotes is very high (≈ 0.8) that may be taken as an indication of the spiral nature of this galaxy.

An important aspect in the images presented in Figures 2 and 3 is the relative brightness among the galaxies. Galaxy A is the brightest galaxy in all optical and J images. However, Galaxy B is brighter than Galaxy A in the K' band. We quantify this in the next section.

3.2. Optical and Near IR photometry

In Table 1 we present our optical and near-IR photometric (absolute magnitudes) results for Galaxies A, B, and C. These were obtained within a circular aperture of $6''$ in order to avoid a possible overlap the disks of galaxies. The second row in Table 1 shows the values from 2MASX total near-IR photometry for Galaxies A and B.

From our own results and those of the 2MASX we observe that Galaxy B is always brighter than Galaxy A, and increases its luminosity at mid-infrared wavelengths. The values presented in Ta-

ble 1 confirm what we observed in the broad band filters: the increase of IR luminosity for Galaxy B.

Using flux calibration in the R filter, we were able to compute an estimate for the $H\alpha$ luminosity value for the A and B galaxies. It is assumed that the flux in the broad band R filter stems from continuum emission. We obtained that the emission from $H\alpha$ is ~ 1.3 and 2 times greater than the continuum for Galaxies A and B, respectively. This indicates, with some confidence, that the $H\alpha$ emission is coming from an HII region in Galaxy A and B. The $H\alpha$ luminosity for Galaxy A and B is estimated to be ~ 3.2 and $\sim 6.4 \times 10^{10} L_{\odot}$, respectively.

4. DISCUSSION

Considering the published redshift for this IRAS source, the projected separation between the center of Galaxy A and B is ≈ 10 kpc. Galaxy C is ≈ 25 kpc away, in projection, from Galaxy A.

Isophotes in Figures 2 and 3 show that Galaxy A is more compact than Galaxy B. In Galaxy B what appears as a tidal feature is observed. This galaxy also shows an increasing luminosity towards the mid-infrared, with an extended emission in the $H\alpha$ wavelength. The extension of this emission is ≈ 8 kpc in projection from side to side.

The $H\alpha$ images show that the most intense emission comes from Galaxy B. This emission is stronger at the edges of a disk-like projected structure than at the central region. This suggests that the central region of Galaxy B contains a significant amount of dust. The previous suggestion is further supported by noticing that the emission peak in the K' filter is located at the central region, where no distortion feature is appreciable; contrary to what is observed in the other filters. Furthermore, such central dust can also explain why the $H\alpha$ emission shows a deficiency in that region, as well as the strong infrared emission.

The large extension of the $H\alpha$ emission in Galaxy B, and its optical broad band filter images, indicate that star formation extends throughout this galaxy. It is highly probable that a large amount of gas is fueling the starburst, which in turn may be due to a tidal interaction with Galaxy A; as is usually observed in interacting galaxies (e.g. Schweizer 1998; Struck 2005).

We may use the relation given by Kennicutt (1998) to compute an estimate of the star formation rate (SFR) from the $H\alpha$ emission. The $SFR(H\alpha)$ for Galaxy A and B are about 2.5 and $5.0 M_{\odot} \text{ yr}^{-1}$, respectively. Also, from the luminosity L_{ir} one may compute (e.g. Kennicutt 1998; Kewley et al. 2002),

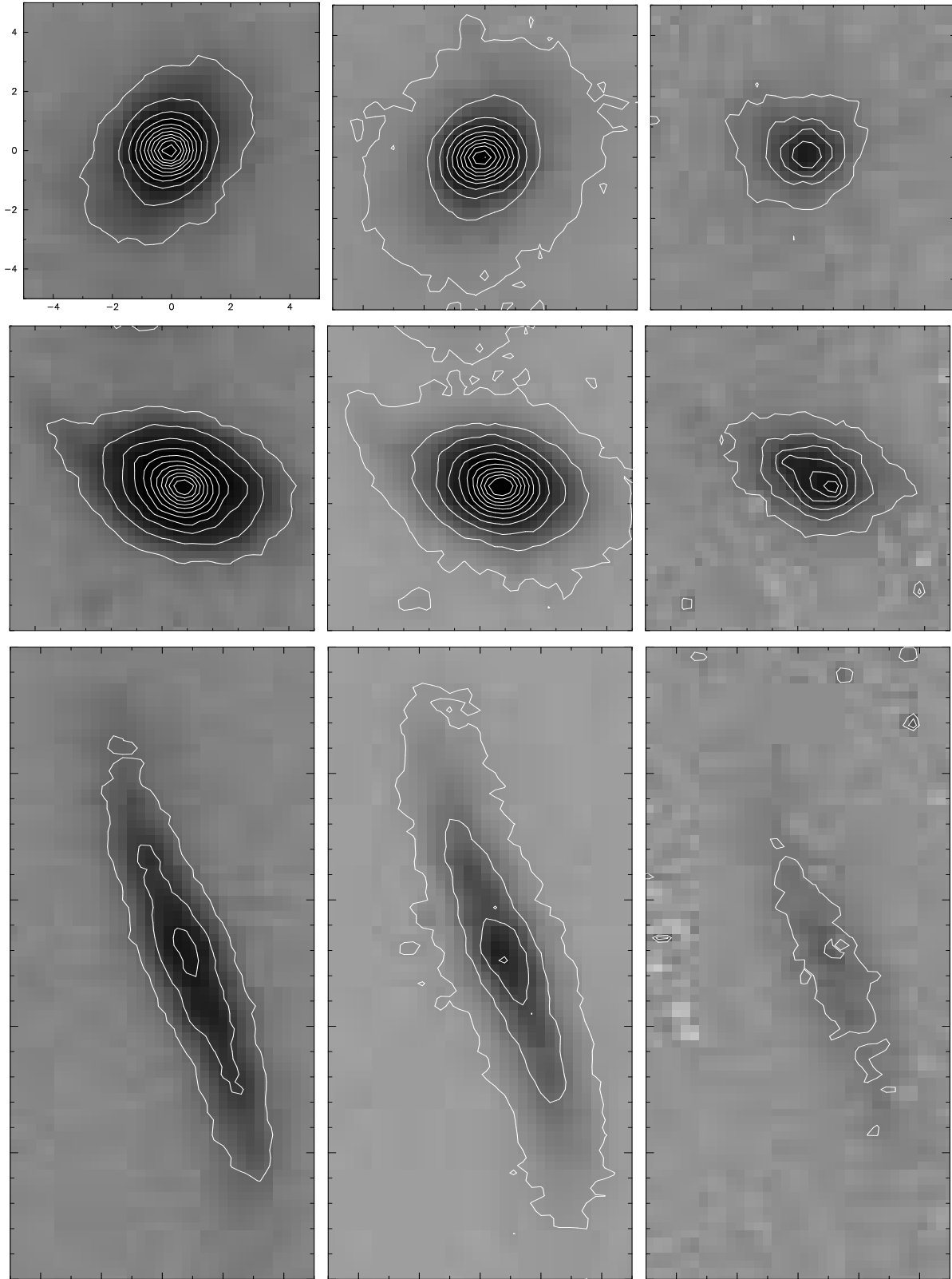


Fig. 3. Near-IR images in J , H and K bands, of the objects labeled A, B and C (from top, middle and bottom, respectively) in Figure 1.

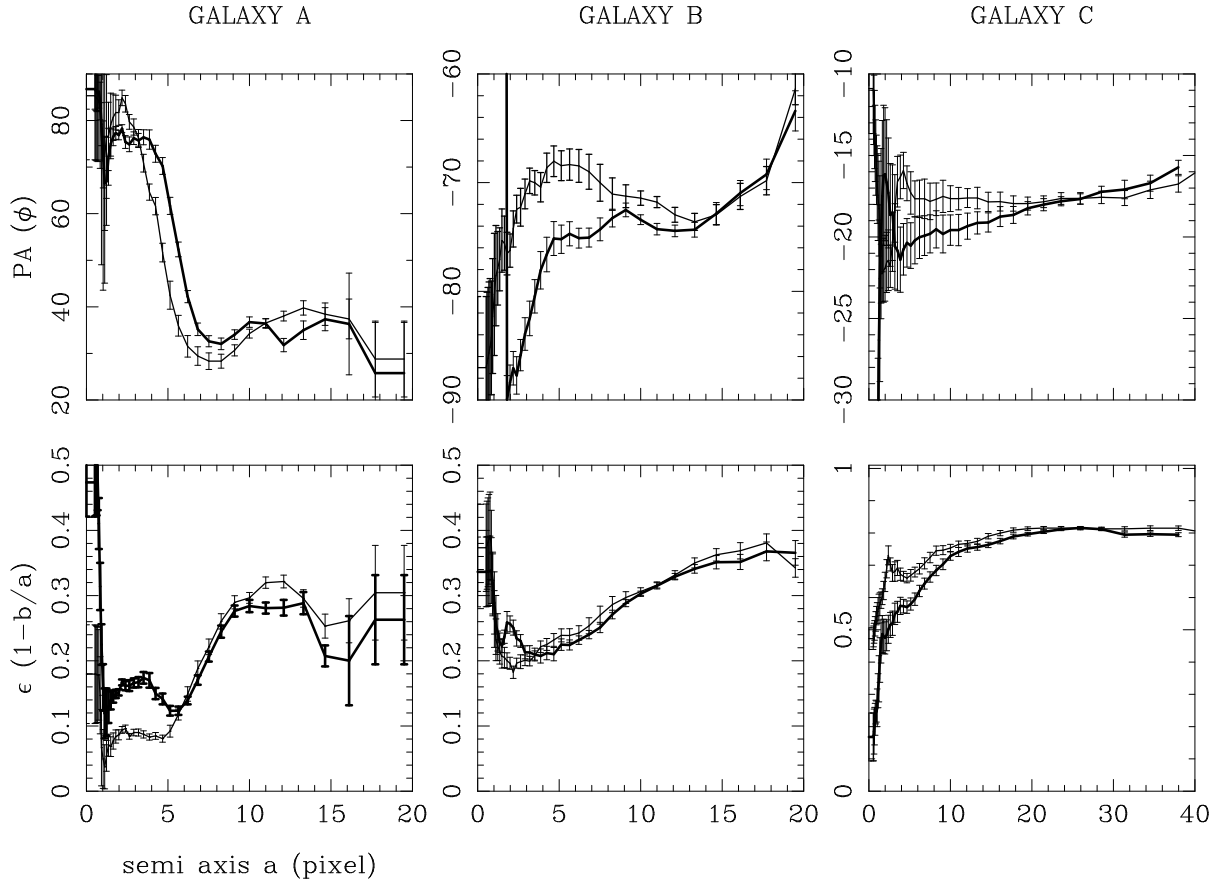


Fig. 4. Ellipticity and position angles for Galaxies A, B and C. Thin lines correspond to the J filter, while thick ones to the H filter.

using the IRAS 60 and 100μ observed fluxes, a $\text{SFR}(\text{IR}) = 73.8 M_{\odot} \text{ yr}^{-1}$ for this IRAS source, i.e. mainly Galaxies A and B.

Using the correlation between infrared to $\text{H}\alpha$ luminosities, without reddening correction $\text{SFR}^*(\text{IR}) = 2.7 \pm 0.3 \text{ SFR}^*(\text{H}\alpha)^{1.3 \pm 0.6}$ (Kewley et al. 2002) and the above results from IRAS flux, we find that $\text{SFR}^*(\text{H}\alpha) = 12.7 M_{\odot} \text{ yr}^{-1}$. The ratio between our $\text{SFR}^*(\text{H}\alpha)$ and $\text{SFR}(\text{H}\alpha)$ is 1.7. So the $\text{SFR}^*(\text{H}\alpha)$ for the A and B galaxies is 3.8 and $7.6 M_{\odot} \text{ yr}^{-1}$, respectively. From these results we conclude that the present IRAS source, Galaxy A and B, are in the expected range for LIRGs galaxies.

All of the features indicated above point towards Galaxy B being probably tidally perturbed by Galaxy A, and this being the reason for the starburst activity inferred by its observed large infrared brightness. Galaxy B, hence, can be identified as the IRAS source. Observations of interacting pair of galaxies (e.g. Xu & Sulentic 1991) show that one galaxy is usually the brightest in infrared emission; this seems to be the case for Galaxy B.

Based on the observations reported here, Galaxy B has a dusty nucleus and a galaxy-wide starburst, and can constitute an example of a LIG galaxy; where the initial infrared phase is triggered during the initial stage of galaxy merger with a companion (e.g. Sanders & Mirabel 1996).

If we consider the IRAS system as composed of a triplet of galaxies (A, B, and C) a projected harmonic-radius (e.g. Aceves 2001) $R_{\text{H}} \approx 27$ kpc follows, assuming the separation between Galaxy C and B to be ≈ 30 kpc. This value of R_{H} is lower than the mean value for the Karachentsev's triplets (e.g. Karachentsev, Karachentseva, & Lebedev 1989; Karachentsev 2000) of $R_{\text{H}} \approx 65$ kpc, making it a rather compact triplet system. Unfortunately, no information about the bulk velocities of each galaxies in the IRAS 02290+2533 source is available, and no direct time-scale for merging can be estimated. Nonetheless, assuming a typical velocity dispersion for triplets ($\sigma \approx 120 \text{ km s}^{-1}$), a value for the crossing time of $t_c = 2R_{\text{H}}(\sqrt{3}\sigma)^{-1} \approx 0.3$ Gyr results.

It highly probable that in this IRAS system a merger will occur in a time-scale $\lesssim 1$ Gyr, and at the moment it can be considered a pre-contact merger system and LIRG system (e.g. Surace et al. 2000). Whether a binary or triple merger is to be expected, is more difficult to state since no information about the orbital parameters of the system can be assessed. However, we expect that a binary merger between Galaxy A and B will occur within the order of one gigayear.

We thank Michael Richer (OAN-SPM) for providing very helpful comments that clarified some topics, also Luis Salas (OAN-SPM) is thank for his input. An anonymous Referee is thanked for his/her comments that help improve the presentation of this work.

REFERENCES

- Aceves, H. 2001, *MNRAS*, 326, 1412
 Armus, L., Heckman, T., & Miley, G. 1987, *AJ*, 94, 831
 Canalizo, G., & Stockton, A. 2001, *ApJ*, 555, 719
 Carico, D. P., Graham, J. R., Matthews, K., Wilson, T. D., Soifer, B. T., Neugebauer, G., & Sanders, D. B. 1990, *ApJ*, 349, L39
 Carrasco, L., García-Barreto, A., Recillas-Cruz, E., Cruz-González, I., & Serrano, A. 1991, *PASP*, 103, 987
 Cruz-González, I., et al., 1994, *RevMexAA*, 29, 197
 Dasyra, K. M., et al. 2006, *ApJ*, 638, 745
 Genzel, R., Tacconi, L. J., Rigopoulou, D., Lutz, D., & Tecza, M. 2001, *ApJ*, 563, 527
 Hopkins, P. F., Somerville, R. S., Hernquist, L., Cox, T. J., Robertson, B., & Li, Y. 2006, *ApJ*, 652, 864
 Karachentsev, I. D. 2000, in *ASP Conf. Ser.* 209, *Small Galaxy Groups*, ed. M. Valtonen & C. Flynn (San Francisco: ASP), 1
 Karachentsev, I. D., Karachentseva, V. E., & Lebedev, V. S. 1989, *Bull. SAO (Izv. SAO)*, 27, 67
 Kennicutt, R. C., Jr. 1998, *ARA&A*, 36, 189
 Kewley, L. J., Geller, M. J., Jansen, R. A., & Dopita, M. A. 2002, *AJ*, 124, 3135
 Kormendy, J., & Sanders, D. B. 1992, *ApJ*, 390, 53
 Lonsdale, C. J., Diamond, P. J., Thrall, H., Smith, H. E., & Lonsdale, C. J. 2006, *ApJ*, 647, 185
 Lonsdale, C. J., Persson, S. E., & Mathews, K. 1984, *ApJ*, 287, 95
 Lu, N., & Freudling, W. 1995, *ApJ*, 449, 527
 Lutz, D., Veilleux, S., & Genzel, R. 1999, *ApJ*, 517, L13
 Mihos, J. C., & Hernquist, L. 1996, *ApJ*, 464, 641
 Murphy, T. W., et al. 1996, *AJ*, 111, 1025
 Neugebauer, G., Soifer, B. T., Rice, W., & Rowan-Robinson, M. 1984, *PASP*, 96, 973
 Sanders, D. B. 2004, *AdSpR*, 34, 535
 Sanders, D. B., & Mirabel, I. F. 1996, *ARA&A*, 34, 749
 Sanders, D. B., Soifer, B. T., Elias, J. H., Madore, B. F., Matthews, K., Neugebauer, G., & Scoville, N. Z. 1988, *ApJ*, 325, 74
 Schweizer, F. 1998, in *Galaxies: Interactions and Induced Star Formation*, Saas-Fee Advance Course 26, ed. Friedli, D., Martinet, L. & D. Pfenniger (New York: Springer-Verlag), 105
 Soifer, B. T., et al. 1984, *ApJ*, 278, L71
 Strauss, M. A., Huchra, J. P., Davis, M., Yahil, A., Fisher, K. B., & Tonry, J. 1992, *ApJS*, 83, 29
 Struck, C. 2005, arXiv:astro-ph/0511335
 Sulentic, J. 1989, *AJ*, 98, 2066
 Surace, J. A., & Sanders, D. B. 1999, *ApJ*, 512, 162
 Surace, J. A., Sanders, D. B., & Evans, A. S. 2000, *ApJ*, 529, 170
 Surace, J. A., Sanders, D. B., Vacca, W. D., Veilleux, S., & Mazzarella, J. M. 1998, *ApJ*, 492, 116
 Telesco, C. M. 1988, *ARA&A*, 26, 343
 Veilleux, S., Kim, D. C., & Sanders, D. B. 2002, *ApJS*, 143, 315
 Veilleux, S., Kim, D. C., Sanders, D. B., Mazzarella, J. M., & Soifer, B. T. 1995, *ApJS*, 98, 171
 Veilleux, S., Sanders, D. B., & Kim, D. C., 1997, *ApJ*, 484, 92
 ———. 1999, *ApJ*, 522, 139
 Xu, C., & Sulentic, J. W. 1991, *ApJ*, 374, 407
 Yun, M. S., Reddy, N. A., & Condon, J. J. 2001, *ApJ*, 554, 803

Fidel Cruz: Bahía San Quintín 211, Ensenada, B. C., Mexico (fidelcru@gmail.com).

Héctor Aceves: Instituto de Astronomía, Universidad Nacional Autónoma de México, Apdo. Postal 877, 22800 Ensenada, B. C., Mexico (aceves@astro.unam.mx).